2018 7th IEEE International Conference on Biomedical
Robotics and Biomechatronics (Biorob)
Enschede, The Netherlands, August 26-29, 2018

Smart Crutches: Towards Instrumented Crutches for Rehabilitation and Exoskeletons-Assisted Walking

YongQi Felix Chen, *Student Member, IEEE,* Danielle Napoli, Sunil K. Agrawal, *Member, IEEE*, Damiano Zanotto, *Member, IEEE*

***Abstract*— Recording 3D ground reaction forces through instrumented crutches can assist patients undergoing ambulatory rehabilitation as well as help roboticists develop new assistive controllers for their exoskeletons. Current methods to measure the amount of weight a patient exerts on their limbs are either inaccurate, or not feasible outside of ideal laboratory conditions. This paper introduces *Smart Crutches*, an instrumented crutch system capable of measuring the weight that a patient places on his/her lower extremities and providing vibratory feedback in response to the measured weight. The device was calibrated using a motion capture system and force plates. Linear regression and support vector regression (SVR) were used for calibration, and 10-fold cross-validation was applied to estimate the system's accuracy. Results indicate that machine learning regression methods may lead to improved accuracy, but the choice of the kernel function is critical. Gaussian kernel yielded root-mean-square errors (RSME) of 2.5N or less relative to force plates, while other kernel functions produced more inconsistent and less accurate results. Instrumented crutches may be a valid alternative to force plates for estimating ground reaction forces in crutch gait.**

Keywords*— *instrumented crutch, machine learning regression, gait rehabilitation, wearable technology

I. Introduction

In the United States, ambulatory rehabilitation accounts for 86.3% of all outpatient rehabilitation [1]. With the growing costs of healthcare in most developed countries, minimizing the amount of time spent with a doctor or therapist not only reduces the costs for patients and insurance companies, but also increases the number of patients healthcare providers can manage and decreases the costs for the hospital or outpatient clinics. In several medical conditions, the use of a crutch is paramount to a complete rehabilitation. However, crutch gait has been shown to involve a larger amount of energy expenditure than normal walking [2]. Using a crutch for extended periods of time, especially incorrectly, can exhaust a patient.

As the weight is slowly reintroduced to the lower limbs after an injury, the limbs are progressively able to withstand the loads, allowing the patient to make an eventual recovery. Applying too much weight too quickly can cause a malunion. Alternatively, if the patient doesn't introduce enough weight on their lower limbs, the limb may not be able to tolerate high loads properly. Improper use of the crutches can also lead to secondary upper extremity injuries, such as crutch palsy and axillary artery thrombosis [3], [4].

Currently, healthcare providers utilize tactile feedback, body weight scales, and force plates [5] to properly train patients on how to use the crutches throughout their rehabilitation. Tactile feedback calls for the patient to place their foot on the hand or foot of a physical therapist, who will then estimate the weight they are exerting on that extremity and direct them to adjust their weight until it is within a range that will allow for a healthy rehabilitation. This approach, which largely relies on therapists' experience, is prone to errors as large as 20-30% of the target weight [6]. Body weight scales allow the patient to quantify how much weight they are placing on their limbs. However, these scales are not portable and therefore they cannot be used during locomotion, which makes it difficult for the patient to learn the appropriate weight to apply to the limb once he/she walks away[7]. Force plates are more accurate than body weight scales[8], but they share the same limitations in terms of portability. Additionally, the use of force plates involves high operational costs and specialized personnel, which many outpatient clinics cannot afford.

Several recent studies have suggested that rehabilitation exercises augmented with biofeedback can facilitate the recovery of motor function over standard rehabilitation [9]–[14]. In the case of instrumented crutches, vibratory biofeedback can signal when the amount of load applied through a crutch exceeds a safe range, allowing the patient to distribute the proper amount of weight among limbs, thus reducing the risk of secondary injuries.

Instrumented crutches can also inform the design and control of exoskeletons for assistance and rehabilitation [15]. Indeed, these wearable robots often include crutches to help the wearer balance during locomotion. Little is known to date about how users distribute their weight between the machine and the crutches during static and dynamic tasks, and how different control strategies may affect patterns of recovery, outcomes, and the risk of secondary injuries. Instrumented crutches capable of continuously tracking interaction forces and ground reaction forces in the unconstrained environment will enable the development and validation of more accurate models of the human-robot coupled dynamics, which in turn will inform future assistive controllers.

In recent years, a number of prototype instrumented crutches have been proposed by research groups. These

YongQi (Felix) Chen, Danielle Napoli, and Damiano Zanotto (dzanotto@stevens.edu) are with the Wearable Robotic Systems (WRS) Lab, Stevens Institute of Technology, Hoboken 07030 NJ. S. K. Agrawal (sunil.agrawal@columbia.edu) is with the Robotics and Rehabilitation (ROAR) Lab, Columbia University, New York, NY 10027.

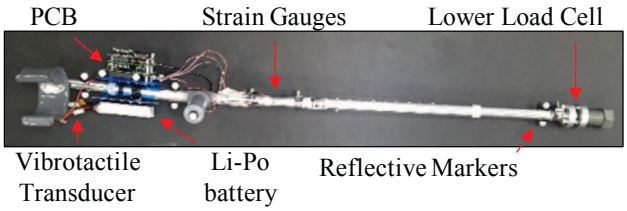

Fig. 1. Prototype of instrumented crutch.

devices are designed to estimate the load that is being exerted on the crutch. Some prototypes do not provide real-time biofeedback [16], [17], and therefore do not offer any advantage in terms of training the patient to a safe and energetically efficient crutch gait. Other systems, such as the one described in [18], can provide auditory feedback. While potentially effective, auditory feedback is obtrusive and can hardly be used during real-life activities, especially in crowded or loud areas.

Some of the proposed prototypes rely on external equipment (e.g., optical motion capture systems) to determine their inclination [17], [19]-[20], which limit their use in real-life environments. Other systems are fully portable and use onboard accelerometers to asses when the crutch has come in contact with the ground [21] or to estimate inclination [16], [18] [22]-[23]. Most of the works which have validated the force estimation capability of instrumented crutches relied on bench testing in static conditions [16], [21], [23], which do not replicate the environment in which the crutches are typically used.

This paper introduces the design of the *Smart Crutches* system and its calibration. The device combines the best traits of past prototypes, being able to determine orientation and 3D ground reaction forces as well as provide vibratory feedback to aid in patient rehabilitation. A new calibration method based on machine-learning regression is shown to improve accuracy and robustness of the system in estimating 3D ground reaction forces.

This paper is organized as follows. Section II details the hardware and software design. Section III provides an overview of the methods used to calibrate the system in dynamic conditions, while Section IV includes the experimental results. These are then discussed in Section V. Conclusion and future plans are presented in Section VI.

II. System Description

The *Smart Crutches* system, shown in Fig. 1, consists of a modified pair of forearm crutches and a control unit. The prototype builds upon a previous device developed at the Columbia University's Robotics and Rehabilitation Laboratory [24] with important updates to the load cell design, electrical design, and software, as detailed below.

The left-crutch and the right-crutch subsystems are identical in design. Each crutch (Medline Industries, Inc., Northfield, IL) was cut just below the handle and next to the bottom tip to house two load cells that measure the bending moments about two orthogonal axes (X and Y axes) and axial forces (along the Z-axis), respectively.

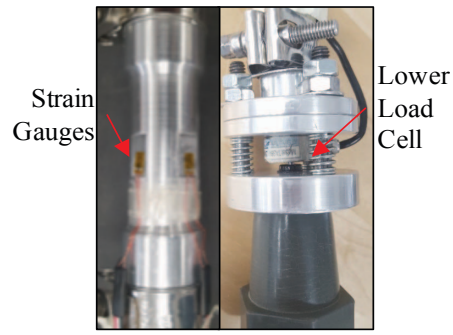

Fig. 2. Upper and lower load cells.

The upper load cell, shown in Fig. 2, consists of two pairs of opposite strain gauges (VPG Inc., Malvern, PA), forming two Wheatstone half-bridges with 350 ohm resistors. The strain gauges are glued on the surface of a custom cylindrical element made out of aluminum alloy, which is secured to the crutch using metal duct clamps. One pair of strain gauges measures moments about the X axis (i.e., the axis along the handle of the crutch, pointing forward) and the other measures moments about the Y axis (i.e., the lateral axis). If the contact with the ground is modeled as a frictionless spherical joint and quasi-static conditions are assumed, then the axial load on the crutch (N) equals the projection of the ground reaction force along Z (R_z) and the bending moments about X (M_x) and Y (M_y) are proportional to the Y and X projections of the ground reaction forces (R_y and R_x), respectively:

$$R_x = -M_y/d,\ R_y = M_x/d,\ R_z = N, \qquad (1)$$

with d being the distance of the strain gauges from the tip of the crutch.

The lower sensor, shown in Fig. 2, is an off-the-shelf single-axis load cell (HT Sensor Technology, Xi'an, China), which is mounted near the base of the crutch, between two aluminum plates that are connected with a system of nuts, screws and pre-loaded compression springs. This custom connection was designed to minimize the sensitivity of the load cell to off-axis loads. The base of the load cell is secured to the top plate with three screws, and the measuring tip of the load cell is in contact with the bottom plate through a stiff rubber washer.

Signals from the top load cells are amplified and filtered by a conditioning board (Mantracourt Electronics Ltd, Devon, UK), digitized by a 12-bit ADC, and sent to an on-board 32-bit microcontroller (PJRC, Oregon, USA) through a SPI port. The bottom load cell signal is conditioned and digitized by a 24-bit ADC board (Sparkfun Electronics, Colorado, US) and

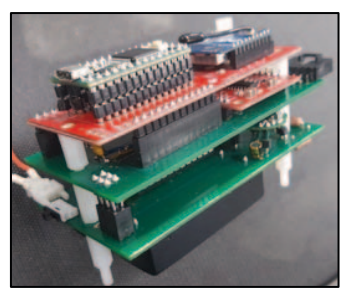

Fig. 3. Printed circuit board configuration

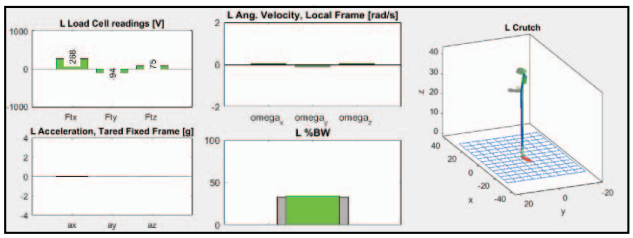

Fig. 4. Matlab Interface for the left crutch

sent to the microcontroller through a serial port. The orientation of each crutch is measured by an on board 9-degree-of-freedom IMU (Yost Labs Inc., Portsmouth, OH). Linear acceleration of the crutch and Yaw-Pitch-Roll angles estimations are sent to the microcontroller through a serial port. All electrical components are assembled on three vertically-stacked printed circuit boards (PCBs), shown in Fig. 3, which are secured above the handle using snap-in fittings. A miniature eccentric rotating mass vibration motor (Yuesui Electron Stock CO) is glued on the back side of the arm cuff to provide bio-feedback. This motor is rated at 3.0V and vibrates at a nominal frequency of 200Hz. The amplitude and timing of the vibrations are controlled through PWM via the on-board microcontroller.

Data is collected at 350 Hz and sent wirelessly using Wi-Fi (IEEE802.11n) to the control unit, a single-board computer (Hardkernel co., Ltd. GyeongGi, South Korea) running a Linux distribution with real-time kernel. The client on each crutch consists of two components, the 32-bit microcontroller and a slave WiFi module (Digi International Inc., Minnetonka, MN). The microcontroller receives and processes all signals from external sensors and relays them to the Wi-Fi module via hardware serial connection. The Wi-Fi module is pre-configured to communicate with the server using the Universal Datagram Protocol (UDP) via Wi-Fi. The same data are also streamed to a graphical user interface (GUI) running on the experimenter's laptop, shown in Fig. 4. The GUI is written in MATLAB (The MathWorks, Natick, MA,USA), and allows the experimenter to control the device remotely and to monitor the device's parameters (i.e., orientation, acceleration, angular velocity, 3D ground reaction forces, and percentage of the subject's body weight applied through each crutch).

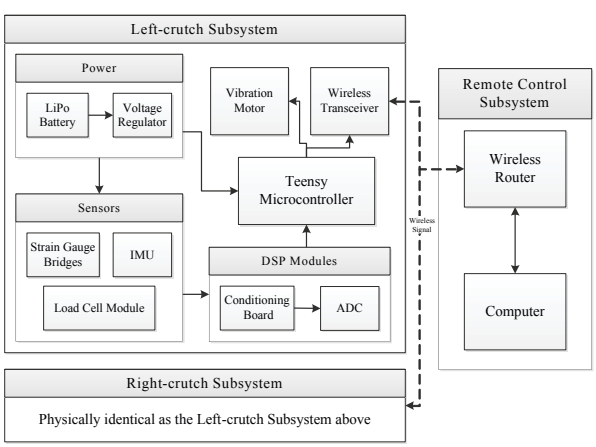

Fig. 5. System Architecture

Fig. 6. Experimental setup showing a crutch pushing against a force plate

The crutches are fully-portable, and each is powered by a 11.1V, 2000mAh Li-Po battery located above the crutches handle, next to the PCB. This battery allows the system to operate continuously for up to 2 hours. The overall architecture of the proposed system is depicted in Fig. 5.

III. Methods

The aim of this calibration procedure was to establish accuracy of the system in estimating ground reaction forces along the X, Y, and Z axes. To this end, force data were simultaneously collected by the on-board load cells and by reference laboratory equipment. Ground-truth data were used to calibrate the portable system using two alternative regression techniques: multivariate linear regression and a learning-based method. Accuracy was estimated with 10-fold cross-validation, using the root-mean-square error (RMSE), the standard deviation of the error (SD) and the coefficient of determination (R^2) as performance metrics.

(A) Experimental Protocol

Calibration of the system was performed using an 8-camera motion capture system (Vero 2.2, VICON, Oxford, United Kingdom) as well as a ground-level force plate (BERTEC, Columbus, OH, US). Seven reflective markers were attached to the crutch to track its motion, as shown in Fig. 1; two towards the upper part of the crutch, two above the handle, one on the tip of the handle, and two just above the lower load cell. To align data from laboratory equipment with those measured by the crutch, a custom-made, wireless sync board with infra-red LEDs was used.

Experiments consisted of three trials, each including two loading cycles performed by one subject. Each trial was designed to primarily excite one component of the ground reaction force. To excite the off-axis force components, the subject tilted the crutch to the left/right, as well as the front/back and applied a variable downward force (Fig. 6). To approximately repeat the loading cycles, the subject could visualize the magnitude of the raw force measured along each direction from the GUI shown in Fig. 4, which was projected on a computer screen.

(B) Data Analysis

Prior to applying regression analysis, data from the force plates and from the on-board load cells were zeroed. Then, the ground reaction forces measured by the force plates were mapped to the crutch local frame using marker data. Data from the force plates were down sampled and aligned with those of the motion capture system. A lowpass IIR filter (Butterworth, 2nd-order, cut-off at 10Hz) cascaded with an averaging filter (window size of 10 samples) were applied to both dataset to remove high frequency noise.

Regression models were trained with 3 features, i.e., digital readings from both the strain gauge bridges (V_x, V_y) and the bottom load cell (V_z). The simplest regression model tested in this study was a multivariate linear regression model in the form:

$$\begin{bmatrix} R_x \\ R_y \\ R_z \end{bmatrix} = \boldsymbol{\beta} \begin{bmatrix} V_x \\ V_y \\ V_z \end{bmatrix}, \tag{2}$$

where R_x, R_y, and R_z are the reaction forces measured by the reference system, V_x, V_y, and V_z are raw readings from the on-board strain gauges and load cells, and $\boldsymbol{\beta} \in \mathbb{R}^{3\times3}$ is calculated through Ordinary Least Squares (OLS) regression. This calibration model is not computationally demanding and, once trained, can be easily implemented in real-time in a microcontroller. However, it cannot compensate for nonlinear trends in the observations, which can potentially result in large fitting errors.

Machine learning regression can potentially achieve higher accuracy at the expense of higher computational load, longer model training time, and extensive use of memory. Yet, once the model has been trained, it can be implemented in real-time in a microcontroller. We applied Support Vector Regression (SVR) models and tested three commonly used kernels (linear, polynomial, and Gaussian). Unlike other learning-based regression methods such as artificial neural networks (ANN), the complexity of SVR models does not depend on the dimensionality of the input space. Additionally, SVR has superior generalization accuracy and global optimization properties [25]. Since SVR is a non-parametric regression method, it does not make assumptions about the functional form of the correlation between predictors and response variable. SVR maps a vector of input data $\boldsymbol{x}$ to a high-dimensional feature space using a nonlinear transformation to kernel space $\varphi(\boldsymbol{x})$, and then estimates the response variable y as a linear combination in the kernel space:

$$\hat{y} = f(\boldsymbol{x}) = \langle \boldsymbol{w}, \varphi(\boldsymbol{x}) \rangle \tag{3}$$

The weights vector $\boldsymbol{w} \in \mathbb{R}^m$, with m being the dimension of the kernel space, is determined by numerically solving the constrained convex optimization problem

$$\min \frac{\|\boldsymbol{w}\|^2}{2} + C \sum_{i=1}^{N_s} (\xi_i + \xi_i^*), \tag{4}$$

subject to

$$\begin{gathered} y_i - \langle \boldsymbol{w}, \varphi(\boldsymbol{x}_i) \rangle \le \varepsilon + \xi_i^*, \;\; i = 1, \dots, N_s \\ \langle \boldsymbol{w}, \varphi(\boldsymbol{x}_i) \rangle - y_l \le \varepsilon + \xi_i, \;\; i = 1, \dots, N_s \\ \xi_i, \xi_i^* \ge 0, \;\; i = 1, \dots, N_s \end{gathered} \tag{5}$$

where N_s is the number of observations $(\boldsymbol{x}_i, y_i)$ and ε is a user-defined error margin, such that errors of magnitude ε or less are neglected. This parameter can be tuned to avoid overfitting. C is a user-defined regularization parameter that describes the cost of misclassifying data: the higher C, the higher the cost of misclassification, leading to a strict classification of data. The slack variables ξ_i, ξ_i^* determine how many observations outside the error margin ε are tolerated, and both are null if the observation is inside ε. It can be shown that (4) and (5) can be turned into a dual optimization problem, leading to a new formulation for (3):

$$f(\boldsymbol{x}) = \sum_{i=1}^{N_s} (a_i^* - a_i) \cdot \langle \varphi(\boldsymbol{x}_i), \varphi(\boldsymbol{x}) \rangle, \tag{6}$$

Where $a_i^*, a_i \in [0, C]$ are Lagrangian multipliers that determine $\boldsymbol{w}$ from the observations. A key feature of SVR is that explicit knowledge of $\varphi(\boldsymbol{x})$ is not required. This allows to substitute $\langle \varphi(\boldsymbol{x}_i), \varphi(\boldsymbol{x}) \rangle$ in (6) with $K(\boldsymbol{x}_i, \boldsymbol{x})$, an admissible SVR kernel. Common kernel functions include linear kernel (7), polynomial kernel (8) and Gaussian–RBF kernel (9):

$$K_L(\boldsymbol{x}_i, \boldsymbol{x}) = \langle \boldsymbol{x}_i, \boldsymbol{x} \rangle, \tag{7}$$

$$K_P(\boldsymbol{x}_i, \boldsymbol{x}) = (1 + \langle \boldsymbol{x}_i, \boldsymbol{x} \rangle)^q, \tag{8}$$

$$K_G(\boldsymbol{x}_i, \boldsymbol{x}) = \exp\left(-\gamma \left|\left|\boldsymbol{x}_i - \boldsymbol{x}\right|\right|^2\right), \tag{9}$$

where γ is the kernel scale of the Guassian-RBF kernel, which controls the fall-off of kernel value when observations move away from their support vector. The error margin ε, the regularization coefficient C and the kernel scale γ are initialized based on the number of input features and observations, then fine-tuned using a heuristic procedure.

Among these kernels, the Gaussian kernel is expected to perform better for non-linear systems because it has localized and infinite response along the x-axis [26]. However, Gaussian kernel can overfit a limited data set. For this reason, linear and polynomial kernels were also tested, and cross-validation techniques were applied to control for data overfitting. For each kernel, SVR was applied three times, one per each projection of the ground reaction forces measured by the reference system: R_x, R_y, or R_z. In all three models, the predictors were the raw readings V_x, V_y, and V_z. All regression models were tested with 10-fold cross-validation. First, the complete dataset was randomly split into ten bins, then, 10 independent regression models were trained by excluding one of the bins each time, and each model was tested on the remaining bin for accuracy. RMSE, R^2, and SD were used to determine goodness of fit of each model, and final error metrics were obtained by averaging the performance of all models.

IV. Results

Table 1 shows the results of the regression models, while Fig. 7 (a-f) reports correlation plots and Bland-Altman plots for the best performing model.

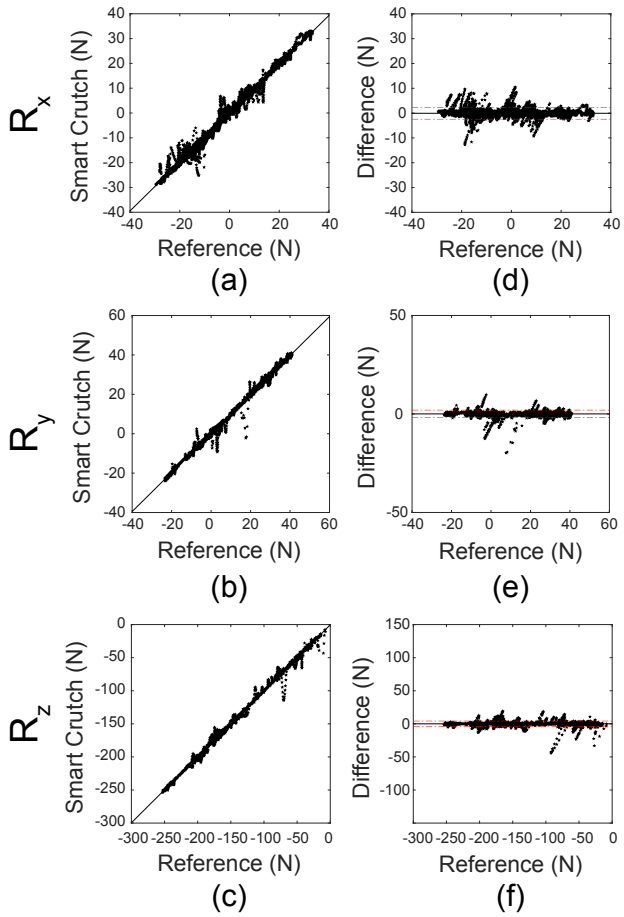

Fig. 7. Correlation plots (a-c) and Bland-Altman plots (d-f) for the SVR model with Gaussian kernel. Red dashed lines indicate 95% limit of agreement.

Linear calibration performed poorly, suggesting that the input-output relationship cannot be accurately represented by the model in (2). Among the SVR models, the Gaussian kernel yielded the best results: R^2 values are close to unity and the error remains within 2.5 N. This indicates a very good agreement between ground-truth data the estimates obtained with the portable system.

V. Discussion

Results suggest that a simple linear model cannot capture the relationship between internal forces measured in the structure of the crutch and 3D ground reaction forces at the tip of the crutch. While the assumption of linear relationship holds quite well for axial forces (R_z), the same was not true for off-axis forces, which nonetheless are very likely to occur both in steady-state crutch gait (e.g., swing-through gait) and during transitions from sit to stand and vice versa.

To obtain accurate estimates, a non-parametric learning-based model was necessary. Several reasons may have contributed to nonlinearities in our system. Most importantly, the contact between the crutch and the ground occurs at the rubber foot of the crutch, which – for safety reasons – is designed to maximize friction and contact surface. Thus, local bending moments might be generated at the interface

	RSME (N)			R^2 (N)			SD (N)		
	Rx	Ry	Rz	Rx	Ry	Rz	Rx	Ry	Rz
Linear Regression	10.4	15.9	14.1	0.46	0.05	0.94	10.4	15.9	14.1
Linear SVM	9.8	17.4	12.2	0.38	0.96	0.12	10.6	13.1	14.2
Polynomial SVM	10.7	7.1	72.2	0.36	0.96	0.12	10.6	16.3	14.2
Gaussian SVM	1.3	1.0	2.5	0.99	1.00	1.00	1.2	1.0	2.2

Table 1. Performance of the four regression models in terms of RMSE, R^2 and SD.

between the crutch and the ground, which are not accounted for by the simplistic model in equation (1). Additionally, the linear model can only compensate for linear cross-talk among the load cells, which is an oversimplification, given that the response of a load cell to loads that are not aligned with its main axis might be nonlinear. For the lower load cell, this effect was partially accounted for by the special design of its housing.

Among the tuning parameters for the learning-based regression models, the type of kernel was found to impact the outcome significantly more than the others. Because it does not rely on an underlying linear model, SVR regression with Gaussian kernel provided more accurate results at the expenses of increased processing time. Thus, this study suggests that learning-based regression is a viable method to improve the accuracy of instrumented crutches in estimating spatial ground reaction forces.

While several other studies have investigated the practicality and effectiveness of instrumented crutches in both the clinical and research sectors ([16], [19], [22]), very few groups have provided data about the accuracy of their systems. Unlike previous work, we quantified the accuracy of the *Smart Crutches* in estimating 3D ground reaction forces under different calibration models. Additionally, instead of relying on bench testing performed under static conditions ([17], [18], [23]), the training and testing datasets used in this paper were measured during dynamic tasks that resembled the actual crutch gait, and were therefore more representative of the dynamic loading the system will undergo during everyday activity.

VI. Conclusion

This paper presented the design and preliminary validation of novel instrumented crutches capable of measuring 3D ground reaction forces and providing real-time vibro-tactile feedback in response to the user's gait, to help him/her learn safe crutch ambulation. In this work, we focused on validating the capability of the system to reliably estimate ground reaction forces.

To the best of the authors' knowledge, this is the first work to investigate the problem of calibrating the output of instrumented crutches with learning-based regression methods. Yet, this paper presented only a proof-of-concept validation of the system, which focused on the estimation of the ground reaction forces. Future work will include extensive human tests, to verify that vibrotactile feedback can help users modulate their weight distribution during crutch gait.

In the future, we envision that fully-portable systems like the *Smart Crutches* will be used in conjunction with assistive exoskeletons, to enable novel human-in-the-loop control strategies.

VII. Acknowledgments

The authors would like to acknowledge the assistance of all the students involved in this project throughout 2017, especially, Naomi Javitt, Katelyn Alecci, Kely Amegbor, Terez Lebron, Richard Logatto and Mohamed Shokry. We also wish to thank Dr. Paul Stegall at the University of Pennsylvania for the valuable discussions.

VIII. References

[1] H. S. Gill, "The changing nature of ambulatory rehabilitation programs and services in a managed care environment," *Arch. Phys. Med. Rehabil.*, vol. 76, no. 12, Supplement 1, pp. SC10-SC15, 1995.

[2] R. L. Waters, J. Campbell, L. Thomas, L. Hugos, and P. Davis, "Energy costs of walking in lower-extremity plaster casts.," *J. Bone Joint Surg. Am.*, vol. 64, no. 6, pp. 896–899, Jul. 1982.

[3] M. dos R. Basílio *et al.*, "Crutch-related acute arterial thrombosis in upper limb: case report," *J. Vasc. Bras.*, vol. 13, no. 4, pp. 340–344, 2014.

[4] S. Raikin and M. I. Froimson, "Bilateral brachial plexus compressive neuropathy (crutch palsy).," *J. Orthop. Trauma*, vol. 11, no. 2, pp. 136–138, 1997.

[5] J. W. Hustedt, D. J. Blizzard, M. R. Baumgaertner, M. P. Leslie, and J. N. Grauer, "Current Advances in Training Orthopaedic Patients to Comply with Partial Weight-Bearing Instructions," *Yale J. Biol. Med.*, vol. 85, no. 1, pp. 119–125, Mar. 2012.

[6] H. L. Hurkmans, J. B. Bussmann, and E. Benda, "Validity and interobserver reliability of visual observation to assess partial weight-bearing," *Arch. Phys. Med. Rehabil.*, vol. 90, no. 2, pp. 309–313, 2009.

[7] H. V Dabke, S. K. Gupta, C. A. Holt, P. O'Callaghan, and C. M. Dent, "How Accurate Is Partial Weightbearing?," *Clin. Orthop. Relat. Res.*, vol. 421, 2004.

[8] F. B. Gray, C. Gray, and J. W. McClanahan, "Assessing the accuracy of partial weight-bearing instruction," *Am. J. Orthop. (Belle Mead. NJ).*, vol. 27, no. 8, p. 558—560, Aug. 1998.

[9] J. W. Hustedt, D. J. Blizzard, M. R. Baumgaertner, M. P. Leslie, and J. N. Grauer, "Is it possible to train patients to limit weight bearing on a lower extremity?," *Orthopedics*, vol. 35, no. 1, pp. e31--e37, 2012.

[10] J. Hustedt, D. Blizzard, M. Baumgaertner, M. Leslie, and J. Grauer, "Partial weight-bearing compliance is maintained over a 24-hour period following training with a biofeedback device," in *Proceedings of 2012 Challenges in Fracture Care Across Disciplines Conference*, pp. 23–25.

[11] D. H. K. Chow and C. T. K. Cheng, "Quantitative analysis of the effects of audio biofeedback on weight-bearing characteristics of persons with transtibial amputation during early prosthetic ambulation," *J. Rehabil. Res. Dev.*, 2000.

[12] E. Hershko, C. Tauber, and E. Carmeli, "Biofeedback versus physiotherapy in patients with partial weight-bearing," *Am J Orthop*, vol. 37, no. 5, pp. E92--E96, 2008.

[13] Z. Pataky, D. D. L. Rodriguez, A. Golay, M. Assal, J.-P. Assal, and C.-A. Hauert, "Biofeedback training for partial weight bearing in patients after total hip arthroplasty," *Arch. Phys. Med. Rehabil.*, vol. 90, no. 8, pp. 1435–1438, 2009.

[14] E. Isakov, "Gait rehabilitation: a new biofeedback device for monitoring and enhancing weight-bearing over the affected lower limb," *Eura. Medicophys.*, vol. 43, no. 1, p. 21, 2007.

[15] G. Chen, C. K. Chan, Z. Guo, and H. Yu, "A review of lower extremity assistive robotic exoskeletons in rehabilitation therapy," *Crit. Rev. Biomed. Eng.*, vol. 41, no. 4–5, 2013.

[16] M. Lancini, M. Serpelloni, and S. Pasinetti, "Instrumented crutches to measure the internal forces acting on upper limbs in powered exoskeleton users," in *Advances in Sensors and Interfaces (IWASI), 2015 6th IEEE International Workshop on*, 2015, pp. 175–180.

[17] A. B. Liggins, D. Coiro, G. W. Lange, T. E. Johnston, B. T. Smith, and J. J. McCarthy, "The case for using instrumented crutches during gait analysis," in *Bioengineering Conference, 2002. Proceedings of the IEEE 28th Annual Northeast*, 2002, pp. 15–16.

[18] G. V Merrett, M. A. Ettabib, C. Peters, G. Hallett, and N. M. White, "Augmenting forearm crutches with wireless sensors for lower limb rehabilitation," *Meas. Sci. Technol.*, vol. 21, no. 12, p. 124008, 2010.

[19] P. S. Requejo *et al.*, "Upper extremity kinetics during Lofstrand crutch-assisted gait," *Med. Eng. Phys.*, vol. 27, no. 1, pp. 19–29, 2005.

[20] B. A. Slavens, P. F. Sturm, R. Bajournaite, and G. F. Harris, "Upper extremity dynamics during Lofstrand crutch-assisted gait in children with myelomeningocele," *Gait Posture*, vol. 30, no. 4, pp. 511–517, 2009.

[21] M. Lancini, M. Serpelloni, S. Pasinetti, and E. Guanziroli, "Healthcare Sensor System Exploiting Instrumented Crutches for Force Measurement During Assisted Gait of Exoskeleton Users," *IEEE Sens. J.*, vol. 16, no. 23, pp. 8228–8237, 2016.

[22] G. V Merrett, C. Peters, G. Hallet, and N. M. White, "An instrumented crutch for monitoring patients' weight distribution during orthopaedic rehabilitation," *Procedia Chem.*, vol. 1, no. 1, pp. 714–717, 2009.

[23] E. Sardini, M. Serpelloni, and M. Lancini, "Wireless instrumented crutches for force and movement measurements for gait monitoring," *IEEE Trans. Instrum. Meas.*, vol. 64, no. 12, pp. 3369–3379, 2015.

[24] B. Wang, "Research and Development of Ambulation Booster Instrumented Forearm Crutches," Columbia University, 2014.

[25] M. Awad and R. Khanna, *Efficient learning machines: theories, concepts, and applications for engineers and system designers*. Apress, 2015.

[26] G. C. Cawley and N. L. C. Talbot, "On over-fitting in model selection and subsequent selection bias in performance evaluation," *J. Mach. Learn. Res.*, vol. 11, no. Jul, pp. 2079–2107, 2010.